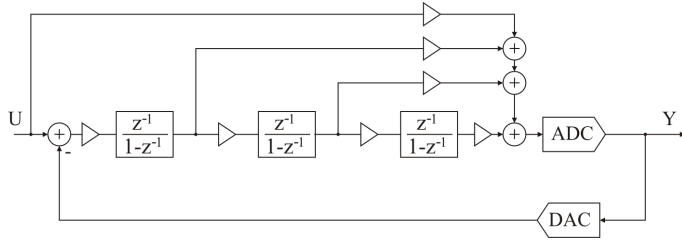
Fig. 2. A block diagram of standard third-order $\Sigma\Delta$ ADC.Fig. 3. A block diagram of third-order feed-forward $\Sigma\Delta$ ADC.

In general, in this case, the Signal Transfer Function (STF) is:

$$STF = \frac{Y(z)}{U(z)} = \frac{H(z)}{1 + H(z)} = z^{-3} \quad (1)$$

which consists of three delays, and the Noise Transfer Function (NTF) is given by:

$$NTF = \frac{Y(z)}{E(z)} = \frac{1}{1 + H(z)} = (1 - z^{-1})^3 \quad (2)$$

In this way, the output signal for the ideal case can be written as:

$$Y(z) = U(z)z^{-3} + E(z)(1 - z^{-1})^3 \quad (3)$$

The output signal has only a pure delay in comparison with the real input signal $U(z)$, while the quantization error $E(z)$ will be pushed out of the output, as it passes through a third-order high-pass filter.

An alternative to standard $\Sigma\Delta$ modulator is an architecture using feed forward paths shown in Fig. 3. The feed-forwards paths are used to enhance a stability of converter, however, the noise transfer function efficiency is reduced.

Analysis of the linearised system shows that assuming an ideal DAC the $\Sigma\Delta$ modulator with the input-feed-forward path has the following signal transfer function:

$$STF = \frac{Y(z)}{U(z)} = \frac{H(z)}{1 + H(z)} = 1 \quad (4)$$

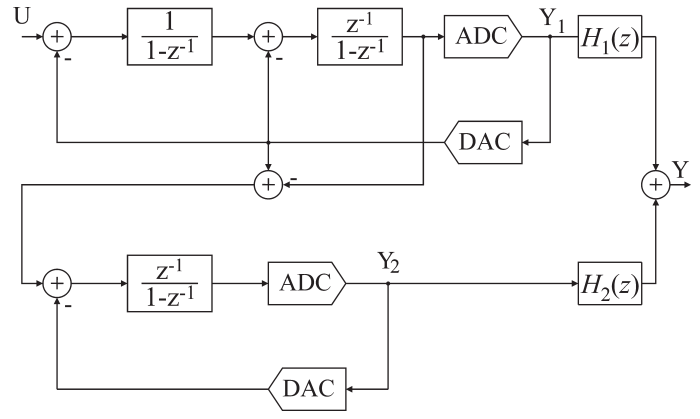
and the noise transfer function:

$$NTF = \frac{Y(z)}{E(z)} = \frac{1}{1 + H(z)} = (1 - z^{-1})^3 \quad (5)$$

the output signal for the ideal case can be written as:

$$Y(z) = U(z) + E(z)(1 - z^{-1})^3 \quad (6)$$

The loop filter $H(z)$ of input feed-forward $\Sigma\Delta$ ADC has to process the quantization noise only, while without the input feed-forward, the loop filter has to process the quantization noise in addition to the input signal. Distortion becomes independent of the input signal, which relaxes linearity requirements. However, the input feed-forward path presents

Fig. 4. A block diagram of third-order two-stage $\Sigma\Delta$ ADC.

a couple of complications, namely the reduced processing time and the analog adder at the quantizer input.

In the $\Sigma\Delta$ modulator without the input feed-forward path, the input-signal and the quantization noise are processed by the loop filter and feed to the quantizer. On the other hand, the input feed-forward path provides an alternate route for the input-signal. The processed quantization noise and the input-signal are then added just before the quantizer. Therefore, the quantizer inputs for both cases are similar. Furthermore, the loop filter is exactly the same for both cases. Therefore, there is no inherent tradeoff between distortion and noise performance in the modulator. The adder at the quantizer input adds thermal noise into the loop. However, noise injected at this point is greatly attenuated when referred back to the input and is therefore insignificant.

A different strategy of high order modulators is to use a multi-stage or MASH (Multi-stAge noise-SHaping) structure of the $\Sigma\Delta$ converter, which relies on the cancellation of the quantization noise. This structure improves the stability problems associated with higher-order modulators.

Using a linear approximation of the modulator in Fig. 4 wherein the quantization is modeled by signal-independent additive error sources, while the integrators are represented by their transfer functions in the z domain. $E_1(z)$ and $E_2(z)$ model the quantization error of the first and second-stage A/D converters, respectively. $E_2(z)$ also contains a representation of nonlinearity in the second-stage A/D converter, and $E_D(z)$ models the error resulting from nonlinearity in the multibit D/A converter in the second stage. A corresponding error source does not appear in the first stage because of the inherent linearity of the 1-b D/A converter. The z transform of the output of the first-stage is:

$$Y_1 = z^{-1}U(z) + (1 - z^{-1})^2 E_1(z) \quad (7)$$

Thus, the output of the first stage includes the input to the modulator delayed by one sample period plus the second-order difference of the first-stage quantization error $E_1(z)$. The input to the second stage is $E_1(z)$ and the transform of the second-stage output is

$$Y_2 = z^{-1}(E_1(z) - E_D(z)) + (1 - z^{-1})E_2(z) \quad (8)$$

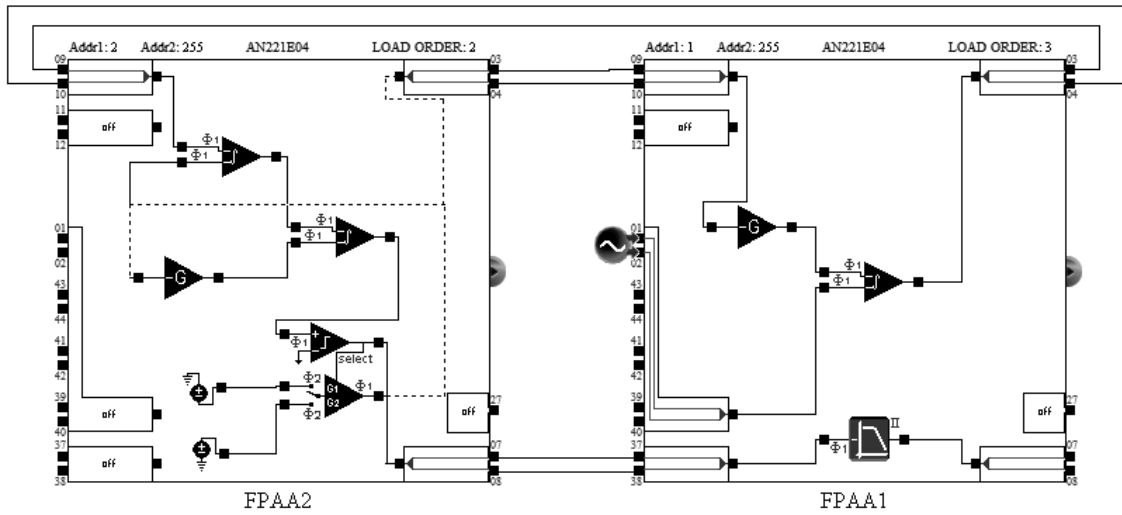


Fig. 5. Circuit realization of the standard third-order $\Sigma\Delta$ ADC.

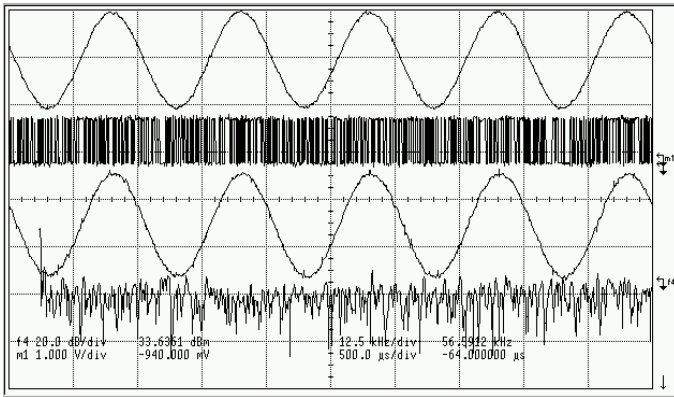


Fig. 6. Sinusoidal input and output waveforms of the standard third-order $\Sigma\Delta$ ADC.

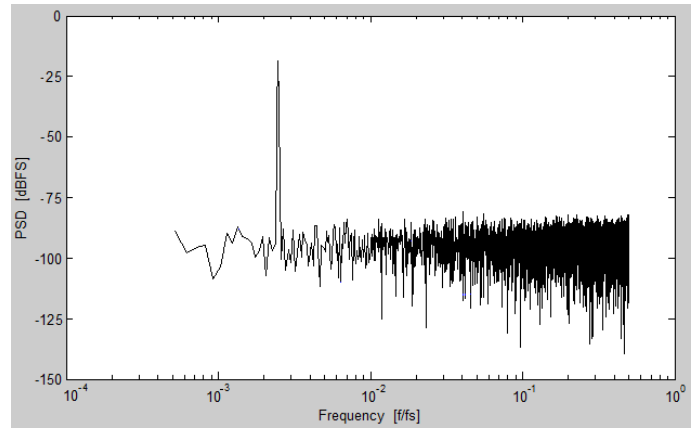


Fig. 8. An output spectrum of the standard third-order $\Sigma\Delta$ ADC excited by 1 kHz input signal.

The error cancellation logic combines the digital outputs from the two stages according to

$$Y(z) = H_1(z)Y_1(z) + H_2(z)Y_2(z) \quad (9)$$

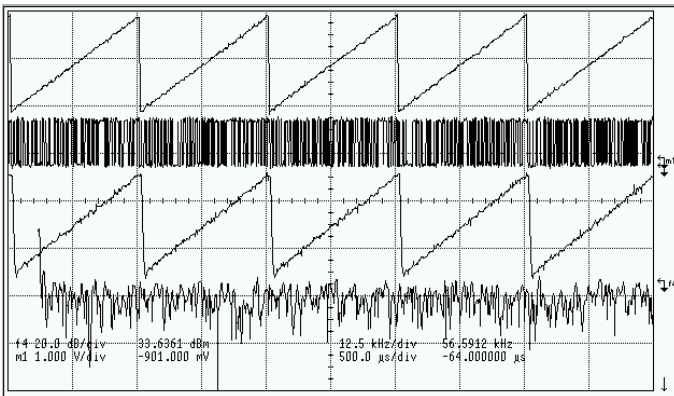


Fig. 7. Linear ramp input and output waveforms of the standard third-order $\Sigma\Delta$ ADC.

In order to cancel the quantization error of the first stage, the digital error cancellation logic is given by the following transfer functions in z plane:

$$H_1(z) = z^{-1} \quad (10)$$

$$H_2(z) = -(1 - z^{-1})^2 \quad (11)$$

The resulting output of the overall modulator is obtained by substituting (7), (8), (10) and (11) into (9) and can be expressed as follows:

$$Y(z) = z^{-2}U(z) + z^{-1}(1 - z^{-1})^2E_D(z) - (1 - z^{-1})^3E_2(z) \quad (12)$$

This is an equivalent of transfer function a standard third-order sigma delta converter, however this structure is stable. The output is now multi-bit, instead of single-bit. Also the cancellation of quantization error requires precise matching of the individual stages. This is challenging for an analog-to-digital converter (ADC). The first stage achieves first-order quantization noise shaping, while the whole modulator

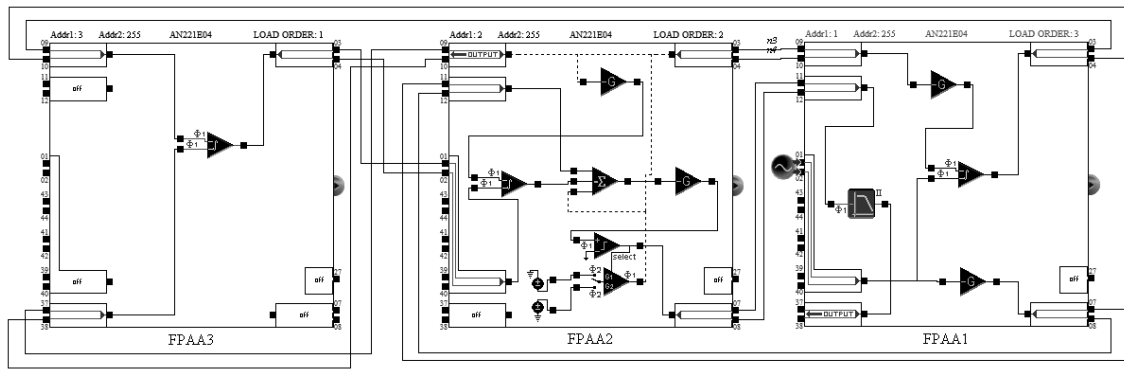


Fig. 9. Circuit realization of the third-order feed-forward $\Sigma\Delta$ ADC.

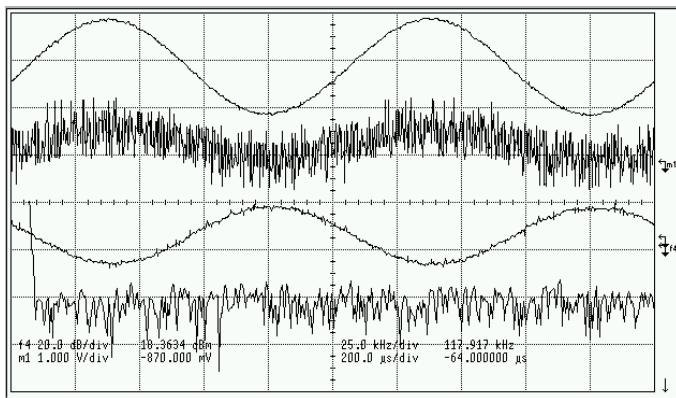


Fig. 10. Sinusoidal input and output waveforms of the third-order feed-forward $\Sigma\Delta$ ADC.

achieves the second order quantization noise shaping of the second stage noise. Provided exact cancellation of the noise from the first stage has been achieved.

III. $\Sigma\Delta$ ADCs IMPLEMENTATION

The standard third-order $\Sigma\Delta$ ADC has been designed and implemented using FPAAs – Anadigm Development Board with three AN221E04 circuits. The prototypes were configured for the following specifications: sampling frequency

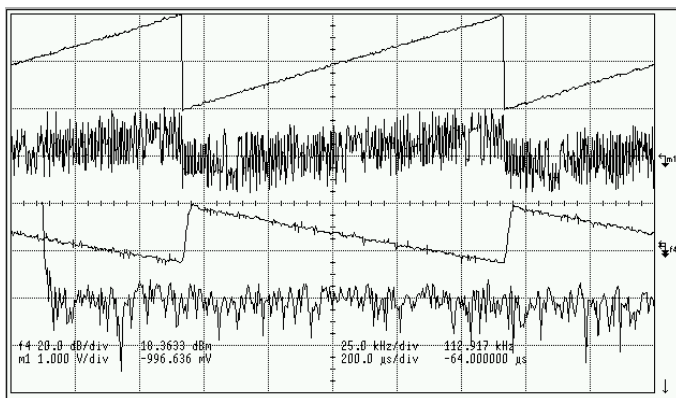


Fig. 11. Linear ramp input and output waveforms of the third-order feed-forward $\Sigma\Delta$ ADC.

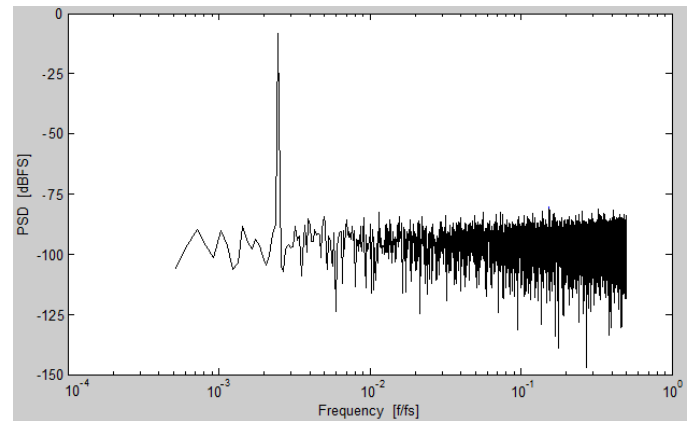


Fig. 12. An output spectrum of the third-order feed-forward $\Sigma\Delta$ ADC excited by 1 kHz input signal.

$f_s = 4\text{MHz}$, bandwidth $BW = 20\text{kHz}$, input signal frequency $f_{in} = 1\text{kHz}$ and oversampling ratio $OSR = 200$. The converter has been designed in AnadigmDesigner2 tool and next programmed at test board, as shown in Fig. 5. Third-order converter has been iteratively reconfigured from pre-calculated structure coefficients to achieve the best performance. Its measured output waveforms for a sinusoidal and for a linear ramp input voltages whose range is between $\pm 3\text{V}$ are shown in Figs. 6 and 7, respectively. The output signals have been achieved by lowpass biquadratic continuous time filtering. Finally a spectrum of the converter excited by the sinusoidal input with amplitude of 1 V pk-pk and a frequency of 1 kHz has been measured and shown in Fig. 8. The measured SNDR (using MATLAB) for a signal bandwidth of 20 kHz is 62.3 dB which is equivalent to 10-bit of resolution.

As shown in Fig. 8, the fundamental problem with this architecture is the noise in the output waveforms. Fortunately, the programmable FPAAs device enables to reconfigure improved converter architecture and to test it very quickly. To improve the noise shaping capability and improve stability in the architecture of the standard third-order $\Sigma\Delta$ ADC shown in Fig. 5, the third-order feed-forward path has been included and then the proposed third-order $\Sigma\Delta$ ADC has been implemented in the FPAAs programmable structure. The third-order feed-forward structure is shown in Fig. 9.

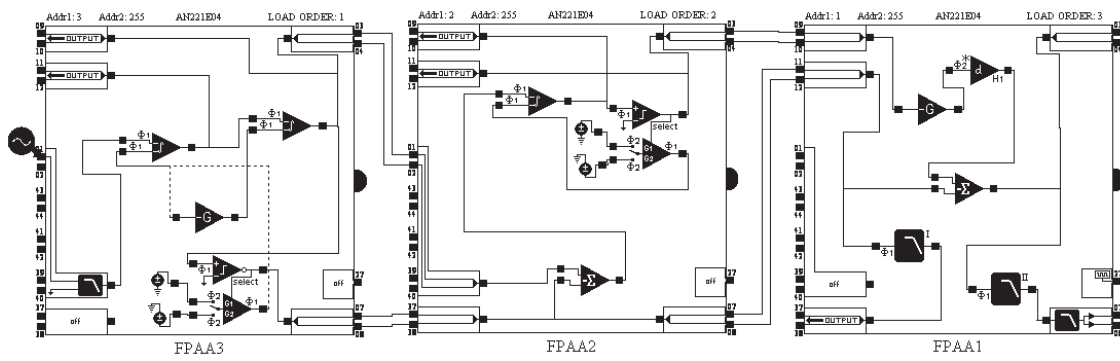


Fig. 13. Circuit realization of the 12-bit third-order multistage $\Sigma\Delta$ ADC.

Measured output waveforms of the third-order feed-forward $\Sigma\Delta$ ADC for a sinusoidal and for a linear ramp input voltages whose range is between $\pm 3V$ are shown in Figs. 10 and 11, respectively. The output signals have been achieved by lowpass biquadratic continuous time filtering.

The $\Sigma\Delta$ ADC achieves the third order quantization noise shaping. The proposed feed-forward third-order converter digital outputs are post-processed in MATLAB, and the achieved SNDR for a sinusoidal input with amplitude of 1 V pk-pk and a frequency of 1 kHz is equal to 71.8 dB or 12 bits in resolution.

A different way to improve the noise shaping capability is using a multi-stage architecture of a third-order $\Sigma\Delta$ ADC, which increase the stability associated with high-order modulators. Two-stages converter has been implemented in the FPAA programmable structure, as shown in Fig. 13. In this converter the noise-shaping performance is essentially that of third-order single-loop converter, but stability behavior is that of a second-order one. This architecture has a direct feed-forward path from the input of the sigma-delta modulator to the ADC input, which results in suppression of the input signal component in the loop-filter. Therefore, the quantization noise is shaped by the integrators, thereby improving the distortion performance.

The third-order multistage $\Sigma\Delta$ ADC has been designed and implemented in FPAA for the following specifications:

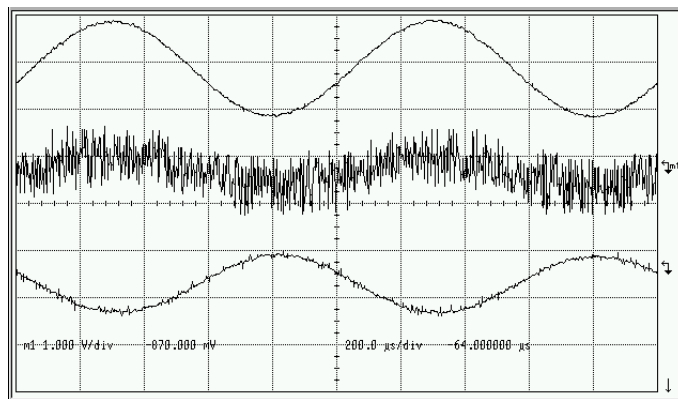


Fig. 14. Sinusoidal input and output waveforms of the 12-bit third-order two-stage $\Sigma\Delta$ ADC.

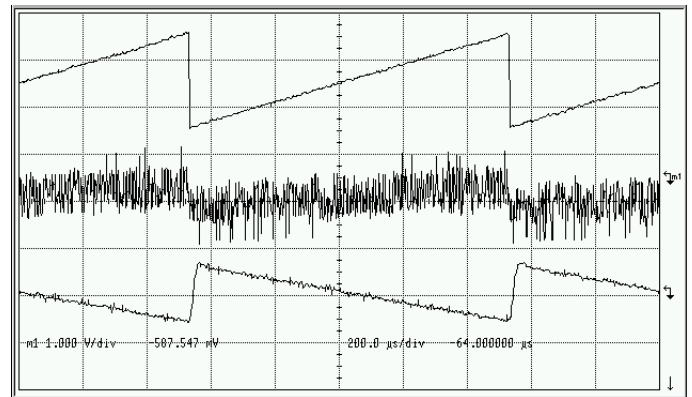


Fig. 15. Linear ramp input and output waveforms of the 12-bit third-order two-stage $\Sigma\Delta$ ADC.

sampling frequency $f_s = 4\text{MHz}$, bandwidth $BW = 20\text{kHz}$ input signal frequency $f_{in} = 1\text{kHz}$ and oversampling ratio $OSR = 200$. Its measured output waveforms for a sinusoidal and for a linear ramp input voltages whose range is between $\pm 3V$ are shown in Figs. 14 and 15, respectively. The output signals have been achieved by lowpass biquadratic continuous time filtering. Finally a spectrum of the converter excited by the sinusoidal input with amplitude of 1 V pk-pk and a frequency of 1 kHz has been measured and shown in

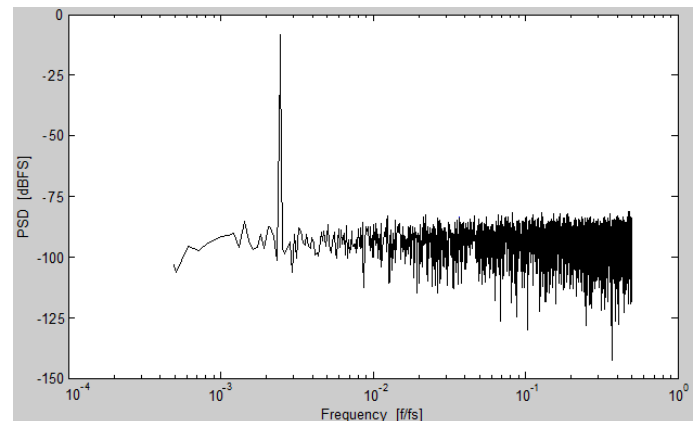


Fig. 16. An output spectrum of the third-order feed-forward $\Sigma\Delta$ ADC.

TABLE I
SUMMARY OF MEASURED PERFORMANCES

| Converter architecture | Standard third-order | Feed-forward third-order | Multistage third-order |
|------------------------|----------------------|--------------------------|------------------------|
| Oversampling ratio | 200 | 200 | 200 |
| Sampling frequency | 4 MHz | 4 MHz | 4 MHz |
| Bandwidth | 20 kHz | 20 kHz | 20 kHz |
| SFDR | 68.4 dB | 76.2 dB | 75.8 dB |
| SNDR | 62.3 dB | 71.8 dB | 70.4 dB |
| Resolution | 10 bits | 12 bits | 11 bits |

Fig. 16. The measured SNDR (using MATLAB) for a signal bandwidth of 20 kHz is 70.4 dB which is equivalent to 11-bit of resolution.

The summary of measured performances and comparison of noise shaping capability of the proposed standard third-order, third-order feed-forward and third-order multistage $\Sigma\Delta$ converters is presented in Table I. Figures 8, 12 and 16 show a FFT spectrum of a 1 kHz signal at a 4 MHz sampling frequency and a 20 kHz bandwidth with an OSR of 200. Spurious-Free Dynamic Range (SFDR) and Signal-to-Noise and Distortion Ratio (SNDR) have been computed and compared. Measured results showed that the third-order feed-forward converter has the best performances. the third-order multistage converter has 1.4 dB worse SNDR, but this architecture is less sensitive to the choice of structural parameters and improves the stability of high-order modulators.

IV. CONCLUDING REMARKS

Prototyping of higher order sigma-delta analog to digital converters has been presented in the paper. The method is based on implementation of FPAA AN221E04 to configure and reconfigure proposed circuits. A third-order $\Sigma\Delta$ ADCs has been considered. In first step the prototyped third-order converter was expanded to a third-order feed-forward architecture which improves the noise shaping capabilities. Next

a multistage architecture was use to improve the stability associated with high-order modulators. Different prototyped structures are shown in Figs. 5, 9 and 13, respectively.

The circuit characteristics have been measured and then structure of the converters have been reconfigured to satisfy input specifications. The power signal density for converters have been computed using MATLAB. The standard third-order converter achieved SNDR 62.3 dB (10 bits), third-order feed-forward achieved SNDR 71.8 dB (12 bits) and third-order multistage achieved SNDR 70.4 dB (11 bits). Measured performances of the reconfigured converters confirm that FPAA reprogrammable devices such as AN221E04 may be useful for rapid and cost effective prototyping of mixed signal systems.

REFERENCES

- [1] R. Suszyński and K. Wawryn, "Prototyping of Higher Order $\Sigma\Delta$ ADC Based on Implementation of a FPAA," in *Proceedings of the International Conference on Signals and Electronic Systems, ICSES*, 2012.
- [2] R. Sarahuja, V. Barcons, L. Balado, and J. Figueras, "Experimental Test Bench for Mixed-Signal Circuits Based on FPAA Devices," in *Proceedings of the 18th Conference on Design of Circuits and Integrated Systems*, 2003, pp. 344–349.
- [3] M. Burns and G. W. Roberts, *An Introduction to Mixed-Signal IC Testing and Measurement*. Oxford University Press, 2000.
- [4] H. Kutuk and S. S. Kang, "Filter design using a new field-programmable analog array (FPAA)," *Analog Integrated Circuits and Signal Processing*, vol. 14, pp. 81–90, 1997.
- [5] Y. Chen and K.-P. Pun, "A 0.5-V 90-dB SNDR 102 dB-SFDR audio-band continuous-time delta-sigma modulator," *Analog Integrated Circuits and Signal Processing*, vol. 71, pp. 159–169, 2012.
- [6] E. Bonizzoni, A. P. Perez, F. Maloberti, and M. A. Garcia-Andrade, "Two op-amps third-order sigma-delta modulator with 61-dB SNDR, 6-MHz bandwidth and 6-mW power consumption," *Analog Integrated Circuits and Signal Processing*, vol. 66, pp. 381–388, 2011.
- [7] H. Roh, H. Lee, Y. Choi, and J. Roh, "A 0.8-V 816-nW delta-sigma modulator for low-power biomedical applications," *Analog Integrated Circuits and Signal Processing*, vol. 63, pp. 101–106, 2010.
- [8] K. Wawryn and R. Suszyński, "Switched current building blocks for sigma-delta modulators," in *Proceedings of the 16th National Conference on Circuit Theory and Electronic Circuits*, 1993, pp. 108–113.